OPEN ACCESS

University of BRISTOL

Sun, H., Pomeroy, J., Baranyai, R., Francis, D., Faili, F., Twitchen, D. J., & Kuball, M. (2016). Temperature-Dependent Thermal Resistance of GaN-on-Diamond HEMT Wafers. *IEEE Electron Device Letters*, *37*(5), 621-624. https://doi.org/10.1109/LED.2016.2537835

Peer reviewed version

Link to published version (if available):
10.1109/LED.2016.2537835

Link to publication record in Explore Bristol Research
PDF-document

This is the author accepted manuscript (AAM). The final published version (version of record) is available online via IEEE at http://ieeexplore.ieee.org/document/7429696/?arnumber=7429696. Please refer to any applicable terms of use of the publisher.

University of Bristol - Explore Bristol Research
General rights

This document is made available in accordance with publisher policies. Please cite only the published version using the reference above. Full terms of use are available:
http://www.bristol.ac.uk/red/research-policy/pure/user-guides/ebr-terms/

Temperature dependent thermal resistance of GaN-on-diamond HEMT wafers

Huarui Sun, James W. Pomeroy, Roland B. Simon, Daniel Francis, Firooz Faili, Daniel J. Twitchen, and Martin Kuball, *Member, IEEE*

***Abstract* – The thermal properties of GaN-on-diamond HEMT wafers from 25 °C to 250 °C are reported. The effective thermal boundary resistance between GaN and diamond decreases at elevated temperatures due to the increasing thermal conductivity of the amorphous SiN_x interlayer, therefore potentially counteracting thermal runaway of devices. The results demonstrate the thermal benefit of GaN-on-diamond for HEMT high power operations, and provide valuable information for assessing the thermal resistance and reliability of devices.**

***Index Terms*—GaN-on-diamond, HEMT, reliability, thermal resistance, temperature dependence.**

I. Introduction

AlGaN/GaN high electron mobility transistors (HEMTs) have revolutionized microwave applications with demonstrated power densities as high as 40 W/mm [1], and frequencies greater than 300 GHz [2]. However, self-heating is still a limiting factor and major concern for device reliability. SiC is used as a standard substrate material for AlGaN/GaN microwave HEMTs and has a thermal conductivity of 330–490 W/mK. To increase the operational power density, diamond that has a ~ 4× higher thermal conductivity is being explored as an efficient heat spreading substrate for GaN HEMTs. The latest GaN-on-diamond technology has demonstrated a three-fold increase in power density compared to GaN-on-SiC wafers [3,4]. However, for any GaN heteroepitaxy, an effective thermal boundary resistance (TBR_{eff}) exists between the GaN device layer and the substrate (SiC, Si, diamond, etc.), which includes contributions from the interfacial layers, the intrinsic thermal resistances at material boundaries, and crystal defects near the interfaces. The TBR_{eff} can be a significant thermal barrier for heat transfer from the GaN HEMT to the diamond substrate; moreover, its temperature dependence is an important factor for consideration in device design and reliability assessment. It has been previously reported that the TBR_{eff} of GaN/AlN/SiC increases substantially with temperature [5], whereas another study suggested only a moderate increase in TBR_{eff} for both GaN/AlN/SiC and GaN/AlN/Si from 300 K to 550 K [6]. In both of these, the TBR_{eff} is effectively dominated by the AlN nucleation layer, which has a decreasing thermal conductivity with temperature due to phonon-phonon scattering and lattice imperfection scattering. This, on top of the decreasing thermal conductivity of the GaN layer and the substrate as a function of temperature, will potentially contribute to device thermal runaway at high power density operations. For GaN-on-diamond, in comparison, the temperature dependence of $TBR_{GaN\text{-}dia}$ plays an even more important role as it accounts for a greater percentage of the total thermal resistance due to diamond's much higher thermal conductivity. The GaN-on-diamond wafers characterized in this work incorporates an amorphous SiN_x interlayer between GaN and diamond. Here we report the measurement of the thermal resistance at the GaN/SiN_x/diamond interface and the effective thermal conductivity of the diamond substrate from 25 °C to 250 °C using nanosecond transient thermoreflectance, and correlate the results with the properties of the amorphous SiN_x layer and the thin nanocrystalline diamond near the nucleation surface. Implications of the temperature dependent thermal properties on the transistor thermal resistance are discussed.

II. Samples and Measurement

The GaN-on-diamond wafers originated from 0.7 μm-thick AlGaN/GaN epilayers grown on Si. The Si substrate was removed, and a ~ 40 nm-thick amorphous SiN_x layer was subsequently deposited on the exposed GaN surface using low-pressure chemical vapor deposition (CVD), followed by the microwave plasma CVD growth of 100 μm-thick polycrystalline diamond. Two samples were characterized: Sample A with a very thin diamond nucleation/transition region (< 10 nm) at the interface, and sample B with a thicker nucleation/transition region (estimated 50–100 nm). This is illustrated by the cross-sectional transmission electron microscope (TEM) images in Fig. 2(a). The variation was controlled by using different seeding methods for the diamond growth. The GaN-on-diamond samples were coated with a 10 nm-thick Cr adhesion layer and then a 150 nm-thick Au film (measured by atomic force microscopy) for the optical measurement.

This work is in part supported by DARPA under Contract No. FA8650-15-C-7517 monitored by Dr. Avram Bar Cohen, supported by Dr. John Blevins, Dr. Joseph Maurer and Dr. Abirami Sivananthan. Any opinions, findings, and conclusions or recommendations expressed in this material are those of the authors and do not necessarily reflect the views of DARPA. HS acknowledges the financial support from EPSRC under Grant No. EP/K024345/1.

Huarui Sun, James W. Pomeroy, Roland B. Simon, and Martin Kuball are with the Center for Device Thermography and Reliability, H.H. Wills Physics Laboratory, University of Bristol, Bristol BS8 1TL, United Kingdom (E-mail: huarui.sun@bristol.ac.uk, martin.kuball@bristol.ac.uk).

Daniel Francis, Firooz Faili and Daniel J. Twitchen are with the Element-Six, Technologies, Santa Clara, CA 95054, USA.

The transient thermoreflectance technique was described in detail in [7,8]: A 10 ns-pulsed 355 nm laser was used to heat the surface of the Au film, inducing a rapid temperature increase. A continuous 532 nm laser was then used to monitor the transient change in the reflectivity of the Au film which is proportional to the temperature rise. The samples were heated in a Linkam thermal stage up to 250 °C. A verified finite element (FE) transient thermal model [4] was used to extract $TBR_{GaN\text{-}dia}$ and the thermal conductivity of the diamond (κ_{dia}) by fitting the measured transients.

III. Results and Discussion

Fig. 1(a) shows measured thermoreflectance transients affected by the $TBR_{GaN\text{-}dia}$ and κ_{dia}; Fig. 1(b) shows the modeled change in the normalized transient with respect to +10% variation in each thermal parameter. The sensitivity shows different magnitudes on different timescales following the spatial and temporal evolution of heat, which diffuses from the gold surface to the GaN layer, and deep into the diamond substrate. The measurement is not sensitive to the thermal conductivity of the Au transducer (κ_{Au}) or the GaN layer (κ_{GaN}) on any distinctive timescale, and hence reported values including their temperature dependencies were assumed for κ_{Au} [9] and κ_{GaN} [6]. The thin AlGaN barrier layer (~20 nm) was included in the lumped thermal resistance between Au and GaN, $TBR_{Au\text{-}GaN}$. Similarly, the SiN_x layer together with the diamond nucleation region and the GaN/SiN_x and SiN_x/diamond interfaces was included in $TBR_{GaN\text{-}dia}$. $TBR_{Au\text{-}GaN}$, $TBR_{GaN\text{-}dia}$, and κ_{dia}, was each obtained by fitting the transients on their respective most sensitive timescales (<100 ns for $TBR_{Au\text{-}GaN}$, 100–500 ns for $TBR_{GaN\text{-}dia}$, and >900 ns for κ_{dia}). Other input parameters for the FE model include the UV laser's spot size and pulse width, the thickness and temperature-dependent specific heat [10,11] of each layer. Representative fitting curves for sample B at different temperatures are shown in Fig. 1(a). From the fits the thermal properties for the two samples were determined at different temperatures.

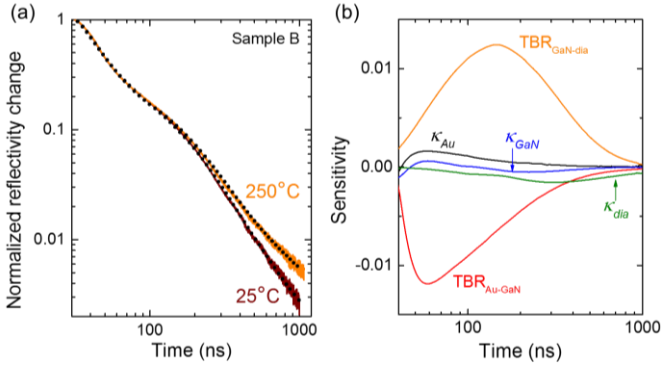

Fig. 1. (a) Measured transients for sample B at 25 °C and 250 °C and corresponding fitting curves. (b) Sensitivity of the thermal transient to different thermal parameters calculated using the finite element thermal model.

Fig. 2(a) shows that $TBR_{GaN\text{-}dia}$ decreases as a function of temperature for both sample A and B. This is in contrast to GaN-on-SiC and GaN-on-Si both having positive temperature dependences of TBR_{eff}. It was previously shown that $TBR_{GaN\text{-}dia}$ is predominantly associated with the amorphous SiN_x [12]. The temperature dependence of $TBR_{GaN\text{-}dia}$ aligns with the increasing thermal conductivity of amorphous dielectrics with temperature [13,14]. Despite having a similar SiN_x thickness, sample B exhibits a consistently greater $TBR_{GaN\text{-}dia}$ compared to sample A at all temperatures, suggesting additional contributions from the thicker nucleation region to the overall interfacial thermal resistance. To separate the different components of $TBR_{GaN\text{-}dia}$, we make two assumptions based closely on the TEM observations (Fig. 2(a) inset). First, as sample A has a negligibly thin nucleation/transition layer, $TBR_{GaN\text{-}dia}$ is presumably dominated by the SiN_x layer, and thus an effective κ_{SiN_x} (including GaN/SiN_x and SiN_x/diamond interfaces) versus temperature was extracted and plotted in Fig. 2(b). The magnitude and temperature coefficient of κ_{SiN_x} may vary depending on the growth, thickness, and the degree of crystallinity/disorder of the SiN_x film [15]. κ_{SiN_x} = 1.6 ± 0.1 W/mK obtained at room temperature is consistent with SiN_x thin films grown by similar methods [15,16]. Secondly, the additional thermal resistance in sample B with respect to A is attributed to the thicker diamond nucleation/transition layer. We can therefore estimate the thermal conductance of the nanocrystalline diamond (NCD) layer. This represents the NCD layer's thermal conductivity per unit thickness (κ_{NCD}/d_{NCD}). As displayed in Fig. 2(b), κ_{NCD}/d_{NCD} is ~ 0.1 GW/m^{2}K and is nearly constant in the measured temperature range. Given the TEM-estimated 50–100 nm thickness for the NCD layer in sample B, this translates to a κ_{NCD} of 5–10 W/mK, consistent with reported thermal conductivities for nanocrystalline diamond films [17]. Due to the presence of the NCD layer, the reduction in $TBR_{GaN\text{-}dia}$ for sample B is only ~ 15% in the measured temperature range, whereas this is ~ 30% for A (as the main contribution is the SiN_x layer). In this case a lower $TBR_{GaN\text{-}dia}$ such as for sample A is more desirable for heat dissipation.

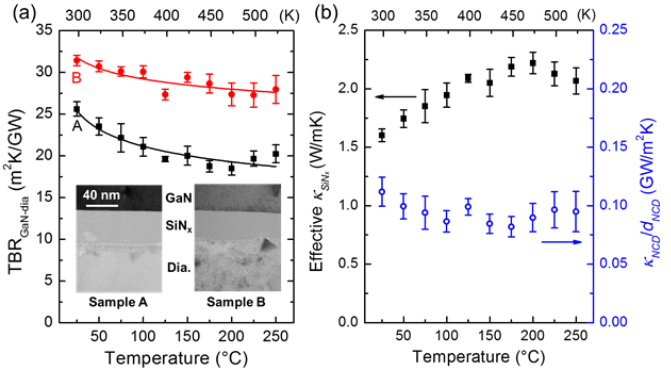

Fig. 2. (a) $TBR_{GaN\text{-}dia}$ versus temperature for sample A and B, respectively. The curves are a guide for the eye. Inset: Cross-sectional TEM images of the GaN/SiN_x/diamond interfaces. (b) Effective thermal conductivity of SiN_x and thermal conductance of nanocrystalline diamond (NCD) extracted from the results in Fig. 2(a).

Due to the columnar growth and coalescence of CVD polycrystalline diamond, strong gradients in the thermal conductivity are present from the nucleation surface towards the growth direction within the diamond [18]. One benefit of the transient thermoreflectance is that it probes the effective κ_{dia} of the diamond as grown on GaN, which represents the spatially weighted average over the 100 μm diamond thickness in the

growth direction. This is the diamond thermal conductivity having the greatest relevance to the device thermal resistance and which is highly dependent on the specific diamond growth conditions and crystal microstructures [19]. As shown in Fig. 3, κ_{dia} decreases with temperature and can be approximated with an empirical expression ~ 1300 $(T/300\text{K})^{-0.9}$ W/mK. For comparison the thermal conductivity for optical grade CVD bulk diamond [20] is also plotted. There is no sizable difference in κ_{dia} between sample A and B, as the only difference between the two samples is the thin nucleation region during the beginning stage of the diamond growth, which was included in $TBR_{GaN\text{-}dia}$. The extracted temperature coefficient of κ_{dia} (–0.9) is greater than that for single crystal SiC (e.g., –1.55 in Ref. 21). This means that the increase in device thermal resistance at elevated temperatures for the diamond used here is less prominent than that for SiC substrate devices. This further favors the use of polycrystalline diamond as the heat spreading substrate, in addition to the decreasing thermal resistance at the interface for GaN-on-diamond devices.

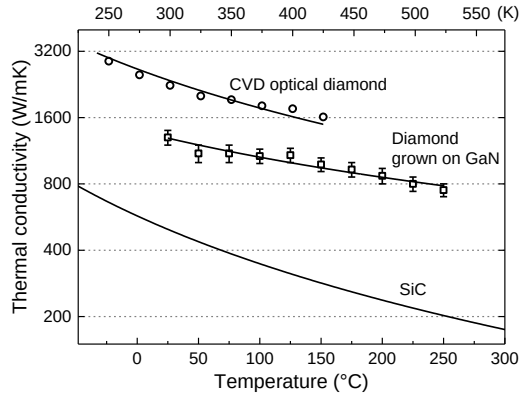

Fig. 3. Effective thermal conductivity of the diamond substrate as grown on GaN. For comparison, temperature dependent thermal conductivities of CVD optical grade bulk diamond [20] and SiC [21] are also included.

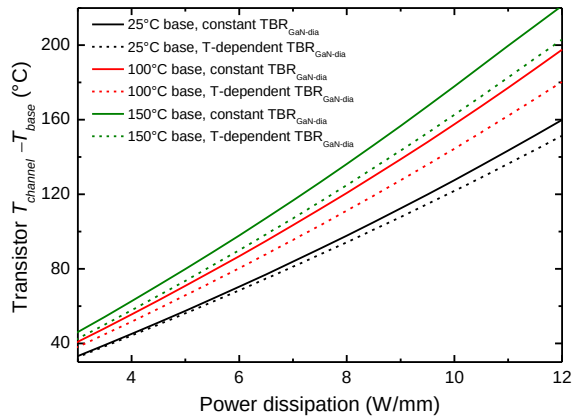

Fig. 4. Modeled transistor channel peak temperature rise at 25 °C, 100 °C, and 150 °C base plate temperatures, with measured temperature dependent and assumed constant $TBR_{GaN\text{-}dia}$ as input, respectively. The transistor consists of 8×125 μm gate width, 43 μm gate pitch, 0.7 μm-thick GaN buffer layer on diamond.

The temperature-dependent thermal properties of GaN-on-diamond HEMT wafers affect the device thermal resistance. To assess this, we use the measured $TBR_{GaN\text{-}dia}$ (of sample A having a lower thermal resistance) and κ_{dia} in a FE transistor thermal model to calculate the channel peak temperature rise ($\Delta T_{channel} = T_{channel} - T_{base}$). The device consists of a typical 8×125 μm gate width, 43 μm gate pitch transistor layout with a 0.7 μm-thick GaN buffer layer on diamond substrate. Fig. 4 shows that the measured $TBR_{GaN\text{-}dia}$, which decreases with temperature, results in consistently lower $\Delta T_{channel}$ than when assuming constant $TBR_{GaN\text{-}dia}$. The difference is greater at higher power dissipations when interface temperatures are raised. This potentially reduces the risk of device thermal runaway, as opposed to the cases of GaN-on-SiC and GaN-on-Si. The effect of the temperature dependent $TBR_{GaN\text{-}dia}$ is more pronounced at elevated T_{base} as often used in RF accelerated life tests, as illustrated in Fig. 4. The difference in $\Delta T_{channel}$ between assumed constant $TBR_{GaN\text{-}dia}$ and measured $TBR_{GaN\text{-}dia}$ is ~ 10% at 100 °C or 150 °C T_{base} with a power dissipation of 12 W/mm. This translates to a difference of one order of magnitude in operating life if we assume a typical activation energy of 1.8 eV for thermally driven wearout [22]. At high temperatures during device operation, the reduced thermal conductivity of GaN causes the in-plane heat dissipation near the device channel to be less efficient, and thus a decreased $TBR_{GaN\text{-}dia}$ is particularly beneficial as it allows the heat to flow more efficiently into the diamond substrate. It should be noted that the critical impact of the diamond substrate on the device electrical performance, as the material originated from a qualified epitaxy (GaN-on-Si), is the lower thermal resistance and thus reduced device channel temperatures. The DC and RF electrical characteristics of related GaN-on-diamond devices were reported in recent publications [23,24], and it was shown [25] that the DC current droop in the saturation region due to self-heating is substantially reduced for GaN-on-diamond HEMTs compared to GaN-on-SiC and GaN-on-Si devices.

In conclusion, the thermal properties of GaN-on-diamond HEMT wafers have been characterized from 25 °C to 250 °C using nanosecond transient thermoreflectance. $TBR_{GaN\text{-}dia}$ decreases with temperature, which is characteristic of the amorphous SiN_x interlayer. The nanocrystalline diamond layer near the nucleation surface also contributes to $TBR_{GaN\text{-}dia}$, and its thermal conductance is estimated to be ~ 0.1 GW/m^{2}K nearly independent of temperature. The effective thermal conductivity of the diamond substrate can be approximated as $\kappa_{dia} \approx 1300\ (T/300\text{K})^{-0.9}$ W/mK. These findings demonstrate the favored thermal properties of GaN-on-diamond compared to GaN-on-SiC and GaN-on-Si over a temperature range relevant for device operations. The temperature dependent thermal properties impact the understanding of GaN-on-diamond HEMTs, and provide essential input for assessing the GaN-on-diamond transistor thermal resistance, especially at high power densities and in RF reliability tests.

REFERENCES

[1] Y. F. Wu, M. Moore, A. Saxler, T. Wisleder, and P. Parikh, "40-W/mm Double Field-plated GaN HEMTs," in *Proc. 64th DRC Tech. Dig.*, 2006, pp. 151–152. DOI: 10.1109/DRC.2006.305162

[2] K. Shinohara, D.C. Regan, Y. Tang, A.L. Corrion, D.F. Brown, J.C. Wong, J.F. Robinson, H.H. Fung, A. Schmitz, T.C. Oh, S.J. Kim, P.S. Chen, R.G. Nagele, A.D. Margomenos, and M. Micovic, "Scaling of GaN HEMTs and schottky diodes for submillimeter-wave MMIC applications," *IEEE Trans. Electron Devices*, no. 60, no. 10, pp. 2982–2996, Oct. 2013. DOI: 10.1109/TED.2013.2268160

[3] J. D. Blevins, G. D. Via, K. Chabak, A. Bar-Cohen, J. Maurer, A. Kane, "Recent progress in GaN-on-diamond device technology," in *Proc. CS MANTECH Conf.*, May 2014, pp. 105–108.

[4] J. W. Pomeroy, M. Bernardoni, D. C. Dumka, D. M. Fanning, and M. Kuball, "Low thermal resistance GaN-on-diamond transistors characterized by three dimensional Raman thermography mapping," *Appl. Phys. Lett.*, vol. 104, no. 8, pp. 083513-1–083513-5, Feb. 2014. DOI: 10.1063/1.4865583

[5] A. Manoi, J.W. Pomeroy, N. Killat, and M. Kuball, "Benchmarking of thermal boundary resistance in AlGaN/GaN HEMTs on SiC substrates: Implications of the nucleation layer microstructure," *IEEE Electron Device Lett.*, vol. 31, no. 12, pp. 1395–1397, Dec. 2010. DOI: 10.1109/LED.2010.2077730

[6] J. Cho, Y. Li, W. E. Hoke, D. H. Altman, M. Asheghi, and K. E. Goodson, "Phonon scattering in strained transition layers for GaN heteroepitaxy," *Phys. Rev. B*, vol. 89, no. 12, pp. 115301-1–115301-1, Mar. 2014. DOI: 10.1103/PhysRevB.89.115301

[7] J. W. Pomeroy, R. B. Simon, H. Sun, D. Francis, F. Faili, D. J. Twitchen, and M. Kuball, "Contactless thermal boundary resistance measurement of GaN-on-Diamond wafers," *IEEE Electron Device Lett.*, vol. 35, no. 10, pp. 1007–1009, Sept. 2014. DOI: 10.1109/LED.2014.2350075

[8] H. Sun, J. W. Pomeroy, R. B. Simon, D. Francis, F. Faili, D. J. Twitchen, and M. Kuball, "Rapid characterization of GaN-on-diamond interfacial thermal resistance using contactless transient thermoreflectance," in *Proc. CS MANTECH Conf.*, May 2015, pp. 151–153.

[9] J. Hartmann, P. Voigt, and M. Reichling, "Measuring local thermal conductivity in polycrystalline diamond with a high resolution photothermal microscope," *J. Appl. Phys.*, vol. 81, no. 7, pp. 2966–2972, Apr. 1997. DOI: 10.1063/1.364329

[10] S. Lee, S. Y. Kwon, and H. J. Ham, "Specific heat capacity of gallium nitride," *Jpn. J. Appl. Phys.*, vol. 50, no. 11S, pp. 11RG02-1–11RG02-3, Nov. 2011. DOI: 10.1143/JJAP.50.11RG02

[11] V. I. Nepsha, "Heat capacity, conductivity, and the thermal coefficient of expansion," in *Handbook of Industrial Diamonds and Diamond Films*, edited by M. A. Prelas, G. Popovici, and L. K. Bigelow, New York, NY: CRC Press, 1997, p. 151.

[12] H. Sun, R. B. Simon, J.W. Pomeroy, D. Francis, F. Faili, D. J. Twitchen, and M. Kuball, "Reducing GaN-on-diamond interfacial thermal resistance for high power transistor applications," *Appl. Phys. Lett.*, vol. 106, no. 11, pp. 111906-1–111906-4, Mar. 2015. DOI: 10.1063/1.4913430

[13] J. J. Freeman and A. C. Anderson, "Thermal conductivity of amorphous solids," *Phys. Rev. B*, vol. 34, no. 8, pp. 5684–5690, Oct. 1986. DOI: 10.1103/PhysRevB.34.5684

[14] S.-M. Lee, D. G. Cahill, and T. H. Allen, "Thermal conductivity of sputtered oxide films," *Phys. Rev. B*, vol. 52, no. 1, pp. 253–257, Jul. 1995. DOI: 10.1103/PhysRevB.52.253

[15] R. Sultan, A. D. Avery, J. M. Underwood, S. J. Mason, D. Bassett, and B. L. Zink, "Heat transport by long mean free path vibrations in amorphous silicon nitride near room temperature," *Phys. Rev. B*, vol. 87, no. 21, pp. 214305-1–214305-9, Jun. 2013. DOI: 10.1103/PhysRevB.87.214305

[16] S. Bai, Z. Tang, Z. Huang, and J. Yu, "Thermal characterization of Si_3N_4 thin films using transient thermoreflectance technique," *IEEE Trans. Ind. Electron.*, vol. 56, no. 8, pp. 3238–3243, Aug. 2009. DOI: 10.1109/TIE.2009.2022078

[17] M. A. Angadi, T. Watanabe, A. Bodapati, X. Xiao, O. Auciello, J. A. Carlisle, J. A. Eastman, P. Keblinski, P. K. Schelling, and S. R. Phillpot, "Thermal transport and grain boundary conductance in ultrananocrystalline diamond thin films," *J. Appl. Phys.* vol. 99, no. 11, pp. 114301-1–114301-6, Jun. 2006. DOI: 10.1063/1.2199974

[18] J. Anaya, S. Rossi, M. Alomari, E. Kohn, L. Tóth, B. Pécz, and M. Kuball, "Thermal conductivity of ultrathin nano-crystalline diamond films determined by Raman thermography assisted by silicon nanowires," *Appl. Phys. Lett.* vol. 106, no. 22, pp. 223101-1–223101-5, Jun. 2015. DOI: 10.1063/1.4922035

[19] J. Anaya, S. Rossi, M. Alomari, E. Kohn, L. Tóth, B. Pécz, K. D. Hobart, T. J. Anderson, T. I. Feygelson, B. B. Pate, and M. Kuball, "Control of the in-plane thermal conductivity of ultra-thin nanocrystalline diamond films through the grain and grain boundary properties," *Acta Mater.* vol. 103, pp. 141–152, Jan. 2016. DOI: 10.1016/j.actamat.2015.09.045

[20] S. E. Coe and R. S. Sussmann, "Optical, thermal and mechanical properties of CVD diamond," *Diamond Relat. Mater.* vol. 9, no. 9–10, pp. 1726–1729, Sept. 1973. DOI: 10.1016/S0925-9635(00)00298-3

[21] G. A. Slack, "Nonmetallic Crystals with High Thermal Conductivity," *J. Phys. Chem. Solids*, vol. 34, no. 2, pp. 321–335, Feb. 1973. DOI: 10.1016/0022-3697(73)90092-9

[22] B. Lambert, J. Thorpe, R. Behtash, B. Schauwecker, F. Bourgeois, H. Jung, J. Bataille, P. Mezenge, C. Gourdon, C. Ollivier, D. Floriot, and H. Blanck, "Reliability data's of 0.5 µm AlGaN/GaN on SiC technology qualification," *Microelectron. Reliab.* vol. 52, no. 9–10, pp. 2200–2204, Sept.–Oct. 2012. DOI: 10.1016/j.microrel.2012.06.098

[23] D. C. Dumka, T. M. Chou, F. Faili, D. Francis, and F. Ejeckam, "AlGaN/GaN HEMTs on diamond substrate with over 7 W/mm output power density at 10 GHz," *Electronics Lett.* vol. 49, no. 20, pp. 1298–1299, Sept. 2013. DOI: 10.1049/el.2013.1973

[24] D. C. Dumka, T. M. Chou, J. L. Jimenez, D. M. Fanning, F. Faili, D. Francis, F. Ejeckam, M. Bernardoni, J. W. Pomeroy, and M. Kuball "Electrical and Thermal Performance of AlGaN/GaN HEMTs on Diamond Substrate for RF Applications" in *Proc. CSICS Conf.*, Oct. 2013, pp. 1–4. DOI: 10.1109/CSICS.2013.6659225

[25] D. C. Dumka and T. M. Chou, "Evaluation of thermal resistance of AlGaN/GaN heterostructure on diamond substrate," in *Proc. ITHERM Conf.*, May 2014, pp. 1210–1214. DOI: 10.1109/ITHERM.2014.6892418